Title	Application of photoelectron spectroscopy to the measurement of the flux of X-ray free-electron lasers irradiationg clusters or biomolecules
Author(s)	Kengo Moribayashi
Citation	Physical Review A,80(2):025403
Text Version	Publisher
URL	http://jolissrch-inter.tokai-sc.jaea.go.jp/search/servlet/search?5019532
DOI	http://dx.doi.org/10.1103/PhysRevA.80.025403
Right	© 2009 The American Physical Society

Application of photoelectron spectroscopy to the measurement of the flux of x-ray free-electron lasers irradiating clusters or biomolecules

Kengo Moribayashi*
Japan Atomic Energy Agency, 8-1 Umemidai, Kizugawa City 619-0215, Japan
(Received 6 January 2009; revised manuscript received 6 July 2009; published 19 August 2009)

This Brief Report shows the behavior of photoelectrons produced by the irradiation of x-ray free-electron lasers (XFELs) onto a cluster or a biomolecule and the measurement of the x-ray fluxes by using the photoelectrons. It is found that plasmas, which are produced through the interaction of XFELs with the target, give little contribution to photoelectrons. The minimum energies of the photoelectrons inform us of the x-ray flux for each target size. Further, these energies approximated by a simple equation agree well with the calculation results for relatively small x-ray fluxes.

DOI: 10.1103/PhysRevA.80.025403 PACS number(s): 32.80.Fb, 33.60.+q

The analysis of the three-dimensional (3D) structures of single biomolecules such as proteins has attracted attention as an application of x-ray free-electron lasers (XFEL) [1–10]. For this analysis, a large number of diffraction patterns produced by the XFEL irradiation of a single biomolecule are needed. Until now, a fixed x-ray flux has been assumed in the theoretical studies [1–4,7,8]. However, since XFELs are focused to a spot size which is comparable with that of a biomolecule in order to get high x-ray fluxes, it is not easy to irradiate the biomolecule with the same x-ray flux for each shot. We need to know the x-ray flux. Therefore, we have been studying how to measure x-ray fluxes irradiating a single biomolecule. For these experiments, it is estimated that a pulse smaller than 5 fs and consisting of about 3×10^{12} photons in a 100-nm-diameter focal spot (an x-ray flux of about 10^{20} photons/pulse/mm^2) is required [1]. In this Brief Report, we treat x-ray fluxes of 10^{18} to 10^{22} photons/pulse/mm^2 and a pulse of 5 fs.

We and our co-workers have proposed a method for the measurement of x-ray fluxes by using the x-ray emission from hollow atoms produced by high x-ray fluxes [10–12]. On the other hand, in this Brief Report, we propose to measure x-ray fluxes by using the energy loss of photoelectrons. It is for this purpose that we study the behavior of photoelectrons for various x-ray fluxes, wavelengths, and sizes of the target. Bostedt *et al.* measured the energy loss of photoelectrons which come from a high-intensity euv laser irradiating Ar clusters [13]. They employed a laser with a wavelength of 32 nm and an intensity of 5×10^{13} W/cm^2 and the target of clusters which consisted of 150 atoms. By using a Monte Carlo simulation, they explained that the space charge in the target is the source of the energy loss. Their simulation model is suitable for small clusters of about 100 atoms. Hau-Riege *et al.* [2], Jurek *et al.* [7], and Ziaja *et al.* [8] also presented the behavior of electrons produced through an XFEL irradiated clusters by using rate equations with the continuum approximation, molecular dynamics based on nonrelativistic classical equations, and hydrodynamics based on the Boltzmann equations, respectively. However, the aims of this Brief Report differ as follows: (i) they focused on the electron movement inside the clusters. (ii) They fixed the x-ray flux. (iii) They calculated the electron energy distribution numerically. However, for the application in the measurement of x-ray fluxes, simple approximation equations between the energy distribution and x-ray fluxes are indispensable. In this Brief Report, we derive simple equations and confirm the agreement of them with the calculation results.

For the measurement of x-ray fluxes, there are other methods such as the use of scattered x rays (which mean x rays scattered by electrons) or the number and degree of ionization of the ions. Since we believe that all of the methods have both advantages and disadvantages for the measurement, we should understand the mechanism of these processes. For example, in the case of scattered x rays, photoelectrons, which can escape from the target, reduce the intensity of the scattered x rays. Furthermore, the interference between x rays scattered through electrons bounded in and ionized from the atoms changes the intensity randomly. The interference comes from the fact that XFELs have full coherence. Therefore, since we forecast that the relationship between the x-ray fluxes and intensity of the scattered x rays becomes nonmonotonic, it is not a simple matter to use the scattered x rays for the measurement. As for photoelectrons, it was thought that the relationship becomes nonmonotonic due to the plasma inside the target. However, in this Brief Report, we will show that the formation of plasma has little effect on photoelectron spectra. We do not intend to say that the use of photoelectron spectra is the only method for the measurement of x-ray fluxes. One should use all the methods mentioned here after understanding each mechanism. Fortunately, we can measure them at the same time.

We treat carbon atom clusters with a spherical shape and at solid density (3×10^{22}/cm^3). The density and number of atoms, which determine the size of the target, may be estimated from other experiments [14]. Our method may be applied to biomolecule targets for the following reasons: (i) as for the shapes of biomolecules, we choose close to spherically shaped biomolecules because of the lack of data concerning their three-dimensional structures. (ii) As for only choosing carbon, the main elements in biomolecules are carbon, nitrogen, and oxygen atoms. However, we do not see a big difference between their atomic data such as cross sec-

*FAX: +81-774-71-3316; moribayashi.kengo@jaea.go.jp

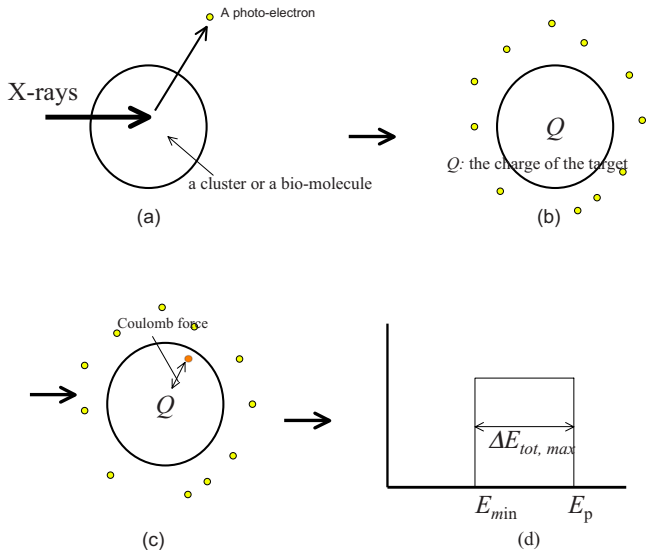

FIG. 1. (Color online) A scenario for the production of photoelectron spectra produced from the interaction of an XFEL with atoms in a cluster or a biomolecule: Figures (a)–(d) are as follows: (a) irradiations of x rays onto the target, (b) production of the charge due to the escape of photoelectrons from the target, (c) the interaction of photoelectrons with the charge, and (d) the outline of the expected photoelectron spectra.

tions and rates in the terms of processes [9,10,15,16]. Figure 1 shows the scenario for the energy loss of a photoelectron. The photoelectrons are produced through x-ray absorption processes, and their initial energies are almost the same as that of various XFELs [see Fig. 1(a)]. The photoelectrons can escape from the target. When one electron escapes, one charge is added. Namely, the space charge (Q) increases according to the number of electrons, which have escaped [see Fig. 1(b)]. The Coulomb force due to this charge reduces the photoelectron energies [see Fig. 1(c)], and the expected spectrum is shown in Fig. 1(d). The total-energy loss (E_p-$E_{\min}$) of the photoelectrons depends on the total charge, which is decided by the x-ray flux, the size and density of the targets, and the energies of the x rays.

Next, we show the theoretical treatment for the behavior of photoelectrons inside and outside the target. We consider not only photoelectrons but also Auger electrons for the calculation of the space-charge Q. Since we assume that the space distribution of the charge becomes almost uniform inside the target as treated in Ref. [2], Q may be considered to be concentrated at the center of the target [9]. The charge affecting an electron [$Q_e(r)$], which is located at a distance of r from the center of the target, is given by $Q_e(r) = \frac{4}{3}\pi r^3 D_{pe} e$, where D_{pe} and e are the density of the photoelectrons and the charge of one electron, respectively. Then, the force acting on the electron is

$$F = \frac{Q_e(r)e^2}{4\pi\varepsilon_0 r^2} = \frac{1}{3\varepsilon_0} r D_{pe} e^2, \tag{1}$$

where ε_0 is the dielectric constant in vacuum. When a photoelectron produced at r escapes from the target, the energy loss of the electron is given by

$$\Delta E(r) = \int_r^{r_0} F dr = \int_r^{r_0} \frac{1}{3\varepsilon_0} r D_{pe} e^2 dr = \frac{1}{6\varepsilon_0} D_{pe} e^2 (r_0^2 - r^2), \tag{2}$$

where r_0 is the radius of the target. Here, we assume that $Q_e(r)$ remains constant from the production to the escape of an electron because it moves too fast for the change in the value of D_{pe}. Then, the averaged energy loss is

$$\Delta E_a = \frac{\int_0^V \Delta E(r) dV}{V} = \frac{\int_0^{r_0} \frac{1}{6\varepsilon_0} D_{pe} e^2 (r_0^2 - r^2) 4\pi r^2 dr}{\frac{4}{3}\pi r_0^3}$$

$$= \frac{1}{15\varepsilon_0} D_{pe} e^2 r_0^2, \tag{3}$$

where V is the volume of the target. Suppose that $r = r_a$ when $\Delta E = \Delta E_a$. Then, from Eqs. (2) and (3), we obtain the following relationship:

$$\frac{1}{15\varepsilon_0} D_{pe} e^2 r_0^2 = \frac{1}{6\varepsilon_0} D_{pe} e^2 (r_0^2 - r_a^2). \tag{4}$$

Namely, $r_a = \sqrt{3/5} r_0$. The energy loss is given by

$$\frac{Q_e(r_0)e^2}{4\pi\varepsilon_0 r_0} = \frac{1}{3\varepsilon_0} r_0^2 D_{pe} e^2 \tag{5}$$

until the electron reaches the detector after the escape. By adding Eq. (3) to Eq. (5), the total-energy loss (ΔE_{tot}) becomes

$$\Delta E_{\text{tot}} = \frac{2}{5\varepsilon_0} r_0^2 D_{pe} e^2. \tag{6}$$

The electrons are produced through ionization processes of atoms or ions such as photoabsorption, Compton scattering, Auger, and electron-impact ionization. In order to count the number of the electrons, we calculate the population of several electronic states due to these ionization processes of C atoms or ions by using rate equations [9–12]. At the same time, D_{pe} can be calculated. We assume that photoionization processes occur at $r = r_a = \sqrt{3/5} r_0$ according to Eq. (4). We employ the rates given in Refs. [9,10,15] where isolated atoms are treated. However, atoms in biomolecules form a condensed-matter system. Therefore, we should compare atomic data of isolated atoms with those of molecules or solids. Some reports [16–19] have shown a comparison of atomic data between condensed matters or molecules and those in isolated atoms. It has been reported that the data of condensed matters or molecules are twice as large as those of isolated atoms at the most.

We have derived a simple approximation equation. In the case where small x-ray fluxes irradiate a target, we may approximate D_{pe} by using $\frac{dN_0}{dt} = -R_{p0} N_0$ and $\frac{dD_{pe}}{dt} = R_{p0} N_0$ [12,20], where N_0 and R_{p0} are the population of the neutral atoms and the photoionization rate for the neutral atom, respectively. Then, N_0 and D_{pe} become

$$N_0 \sim \exp(-R_{p0}t)N_{00}, \quad D_{pe} \sim [1-\exp(-R_{p0}t)]N_{00}, \quad (7)$$

respectively, where N_{00} is the initial density of the neutral atoms. By inserting Eq. (7) into Eq. (6), the total-energy loss is rewritten as

$$\Delta E_{\mathrm{tot}} \sim \frac{2}{5\varepsilon_0} r_0^2 e^2 N_{00}[1-\exp(-R_{p0}t)] = \frac{2}{5\varepsilon_0} r_0^2 e^2 N_{00}\left[1-\exp\left(-\frac{I\sigma_{p0}}{E_p}t\right)\right], \quad (8)$$

with $R_{p0} \sim \frac{I\sigma_{p0}}{E_p}$, where I, σ_{p0}, and E_p are the intensity of the x rays, a photoabsorption cross section for the neutral atoms, and the energy of the x rays, respectively. Furthermore, I is estimated as $I \sim \frac{F_X E_p}{\tau}$, where τ is the pulse length.

Then, at $t=\tau$, ΔE_{tot} becomes maximum, that is,

$$\Delta E_{\mathrm{tot,max}} \sim \frac{2}{5\varepsilon_0} r_0^2 e^2 N_{00}[1-\exp(-F_X\sigma_{p0})]. \quad (9)$$

In order to verify our model given in Fig. 1, we also execute accurate calculations of photoelectron spectra for a small size cluster of a few 1000 atoms by using the Monte Carlo method and Newton's equations (MCN) and compare them with the results calculated by the rate equations. The MCN method employed here is almost the same as that treated in Ref. [7] except for the movements of ions. We do not treat the movements of the ions because the pulse of XFELs treated here is too short for the movement of ions [1]. The following two points should be noted: (i) the production of the electrons depends on the initial seed of the random number generated, which are employed in the Monte Carlo method, that is, we should demonstrate the calculations of photoelectron spectra for different pulses by using different initial seeds for the random number generated. We will show not only the spectra of one pulse but also those averaged by a few tens of pulses. (ii) We consider the effect of the plasma in the target on photoelectron spectra in the MCN method. On the other hand, for the rate equation method, only the energies of the electrons are treated, that is, this effect is ignored.

Figure 2 shows the comparison of the photoelectron spectra calculated by the rate equations and the MCN method. The target radius treated here is 2.5 nm and x-ray flux is 3×10^{20} photons/pulse/mm^2. For the MCN method, not only spectra of one pulse but also those averaged over 30 pulses are shown. Good agreement between them is shown for the minimum energies. This means that the plasma in the target contributes little to the spectra. This may come from the fact that the energy loss after the escape from the target is much larger than that before the escape [see Eqs. (3) and (5)]. It should be noted that the shapes of the spectra shown in Fig. 2 agree well with our expected one shown in Fig. 1(d).

Since it takes too much time to calculate photoelectron spectra for much larger target sizes [7], we employ only the rate equations to calculate the size dependence on the spectroscopy. Figure 3 shows the maximum values of ΔE_{tot} ($\Delta E_{\mathrm{tot,max}}$) as a function of F_X for various values of r_0, a pulse of 5 fs, and (a) $E_p=12$ keV and (b) $E_p=20$ keV. Approximate solutions given by Eq. (9) are also shown. As r_0 increases, the upper limit of the values of F_X, where $\Delta E_{\mathrm{tot\,max}} < E_p$, becomes smaller because $\Delta E_{\mathrm{tot,max}}$ increases according to r_0^2 [see Eq. (6)]. Much larger values of x-ray fluxes can be measured at $E_p=20$ keV than those at

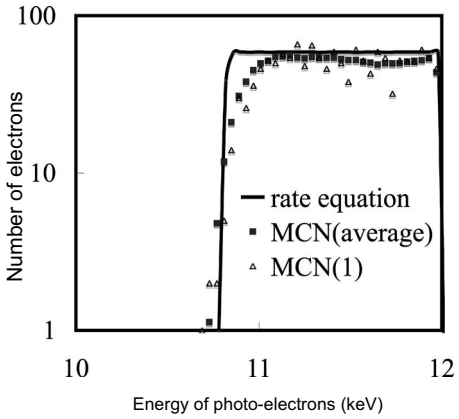

FIG. 2. The comparison of the photoelectron spectra calculated by the rate equation method (solid lines) with those averaged over 30 pulses (solid squares) and those of one pulse (open triangles) by using the Monte Carlo method and Newton's equations (MCN). The target radius treated here is 2 nm. The x-ray flux is 3×10^{20} photons/pulse/mm^2.

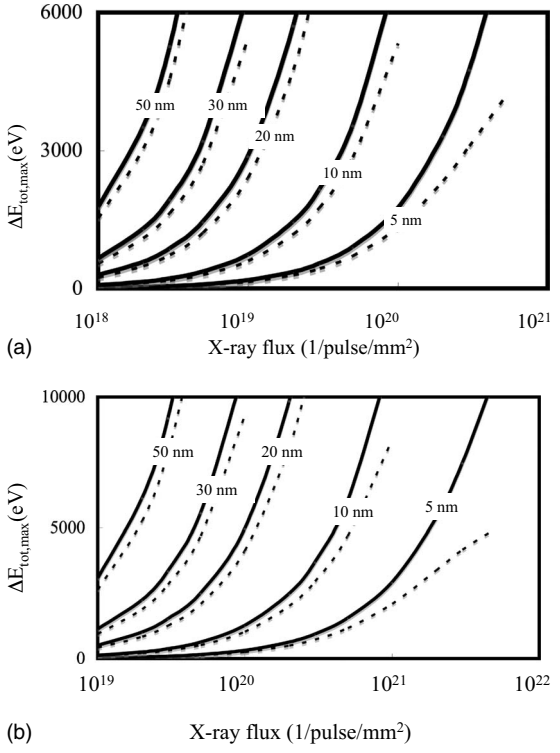

FIG. 3. Maximum values of the energy loss of photoelectrons ($\Delta E_{\mathrm{tot,max}}$) vs x-ray fluxes ($F_X$) for various radii of the target, the pulse of 5 fs, and x-ray energies (E_p) of (a) 12 keV and (b) 20 keV: approximate solutions given by Eq. (9) are also shown. Solid lines: the calculation results, dotted lines: approximate solutions. Radius values of the target are taken to be 5, 10, 20, 30, and 50 nm which are shown in the lines.

$E_p=12$ keV. This comes from the fact that the photoabsorption cross section at $E_p=20$ keV is much smaller than that at $E_p=12$ keV [16] and $\Delta E_{\mathrm{tot,max}}$ depends on σ_{p0} [see Eq. (9)]. The approximation equation is valid at x-ray fluxes smaller than $10^{20}/\mathrm{pulse}/\mathrm{mm}^2$ for $E_p=12$ keV and $10^{21}/\mathrm{pulse}/\mathrm{mm}^2$ for $E_p=20$ keV, respectively, and independent of r_0 where $F_X\sigma_{p0}\ll 1$. We estimate that the error of the approximation equation is within 20%. As F_X increases, the approximations become worse because a larger number of ions are produced. The discrepancy between the calculation and the approximation results mainly comes from the fact that ionization processes from inner-shell excited states and ions produced through Auger processes are ignored in this approximation.

In practice, our model treated here is not satisfactory with regard to the following points: (i) we assume a spherical shape and uniform distribution of the target. (ii) We do not treat ion movement. In order to overcome these drawbacks, we have to make more accurate calculations, for example, by using a molecular dynamic [7], hydrodynamic [8], or a particle-in-cell method [21].

In summary, we have studied the behavior of photoelectrons produced by x-ray free-electron lasers irradiating a cluster or a biomolecule. Considering this property, we have proposed to measure x-ray fluxes irradiating a single cluster or a biomolecule by using photoelectron spectroscopy. It has been found that the formation of plasma gives little contribution to the spectroscopy. Much larger x-ray fluxes can be measured at an x-ray energy of $E_p=20$ keV than that at $E_p=12$ keV. We have derived a simple approximation equation. The equation is valid for x-ray fluxes smaller than 10^{20} photons/pulse/mm^2 for $E_p=12$ keV and 10^{21} photons/pulse/mm^2 for $E_p=20$ keV, respectively, and independent of the size of a cluster or a biomolecule.

We would like to thank Professor Yao (Kyoto Univ.) and Dr. Koga (JAEA) for their useful comments. This study has been supported by the "X-ray Free Electron Laser Utilization Research Project" of the Ministry of Education, Culture, Sports, Science and Technology of Japan (MEXT).

[1] R. Neutze, R. Wouts, D. Spoel, E. Weckert, and J. Hajdu, Nature (London) **406**, 752 (2000).
[2] S. P. Hau-Riege, R. London, and A. Szoke, Phys. Rev. E **69**, 051906 (2004).
[3] S. P. Hau-Riege, R. A. London, H. N. Chapman, A. Szoke, and N. Timneanu, Phys. Rev. Lett. **98**, 198302 (2007).
[4] H. N. Chapman, S. P. Hau-Riege, M. J. Bogan, S. Bajt, A. Barty *et al.*, Nature (London) **448**, 676 (2007).
[5] S. Eisebitt, J. Lüning, W. F. Schlotter, M. Lörgen, O. Hellwig, W. Eberhardt, and J. Stöhr, Nature (London) **432**, 885 (2004).
[6] T. Shintake, Phys. Rev. E **78**, 041906 (2008).
[7] Z. Jurek, G. Faigel, and M. Tegze, Eur. Phys. J. D **29**, 217 (2004).
[8] B. Ziaja, A. R. B. de Castro, E. Weckert, and T. Möller, Eur. Phys. J. D **40**, 465 (2006).
[9] K. Moribayashi and T. Kai, J. Phys.: Conf. Ser. **163**, 012097 (2009).
[10] K. Moribayashi, J. Phys. B **41**, 085602 (2008).
[11] K. Moribayashi, T. Kagawa, and D. E. Kim, J. Phys. B **37**, 4119 (2004).
[12] K. Moribayashi, A. Sasaki, and T. Tajima, Phys. Rev. A **58**, 2007 (1998).
[13] C. Bostedt, H. Thomas, M. Hoener *et al.*, Phys. Rev. Lett. **100**, 133401 (2008).
[14] O. F. Hagena and W. Obert, J. Chem. Phys. **56**, 1793 (1972).
[15] T. Kai and K. Moribayashi, J. Phys.: Conf. Ser. **163**, 012035 (2009).
[16] B. L. Henke, E. M. Gullikson, and J. C. Davis, At. Data Nucl. Data Tables **54**, 181 (1993).
[17] Y. Hatano, Phys. Rep. **313**, 109 (1999).
[18] M. Coville and T. D. Thomas, Phys. Rev. A **43**, 6053 (1991).
[19] M. Neeb, B. Kempgens, A. Kivimäki *et al.*, J. Electron Spectrosc. Relat. Phenom. **88-91**, 19 (1998).
[20] K. Moribayashi, A. Sasaki, and T. Tajima, Phys. Rev. A **59**, 2732 (1999).
[21] Y. Fukuda, Y. Kishimoto, T. Masaki, and K. Yamakawa, Phys. Rev. A **73**, 031201(R) (2006).